Catalysis Communications 65 (2015) 96–101

Contents lists available at ScienceDirect

Catalysis Communications

journal homepage: www.elsevier.com/locate/catcom

Short communication

Cavity-confined acceleration of iron cycle for the Fenton-like reaction by β-CD-benzoquinone host–guest complex under visible irradiation

Liting Fu [a], Zhenwen Zhao [b], Jiahai Ma [a,*], Xuefeng Hu [c,*]

[a] School of Chemistry and Chemical Engineering, University of Chinese Academy of Sciences, Beijing 100049, PR China
[b] Beijing Mass Spectrum Center, Institute of Chemistry, Chinese Academy of Sciences, Beijing 100190, PR China
[c] Key Laboratory of Coastal Environmental Processes and Ecological Remediation, Yantai Institute of Coastal Zone Research, Chinese Academy of Sciences, Yantai, Shandong 264003, PR China

ARTICLE INFO

Article history:
Received 18 December 2014
Received in revised form 30 January 2015
Accepted 9 February 2015
Available online 17 February 2015

Keywords:
Host–guest complex
Iron cycle
Visible irradiation
Fenton

ABSTRACT

The catalyst (CDBQ) that was prepared from β-cyclodextrin (β-CD) and 2,5-dihydroxy-1,4-benzoquinone (2,5-DBQ) achieved the cavity-confined acceleration of iron cycle under visible irradiation. The semi-quinone-like (SQ) radical was generated from photoexcitation of 2,5-DBQ within the β-CD's cavity. The SQ radical as an electron donor could coordinate with iron ions, and thus 2,5-DBQ shuttled one electron between Fe^{3+} and Fe^{2+} via Fe–dihydroxybenzoquinone complex process. In Fenton reactions, CDBQ greatly increased the $HO^{\bullet}$ yield, and thus significantly accelerated the degradation of dyes. The cavity-confined acceleration of iron cycle has promising applications in photo-Fenton system for the efficient decontamination for wastewater.

1. Introduction

There is no doubt that iron plays an irreplaceable role in industrial, chemical and biological systems [1–3]. Fe^{3+} and Fe^{2+} are the dominant forms of iron, and the cycle between them contributes to many significant redox reaction in environmental and chemical systems, for instance, the oxidation of S(IV) to S(VI) [4,5] and the redox cycle of As(III)/As(V) and Cr(III)/Cr(VI) [6,7]. The cycle can also generate and deplete the reactive oxygen species [8–11] and degrade the dissolved organic matter [12,13] in natural water, influencing the global carbon cycle. The redox cycle of Fe^{3+}/Fe^{2+} can be driven by several methods, including photocatalysis [14–16], chemical catalysis [17] and sonoprocessing [18,19]. Hydroquinone/quinone analogues [14,20–22] have also been utilized to accelerate the Fe^{3+}/Fe^{2+} cycle through the reversible conversion of the Q/SQ from the quinone structure unit. The unprotected Q/HQ molecules play the sacrificing co-catalysts to accelerate the iron cycle in that they will be attacked by $HO^{\bullet}$. Consequently, quinones were loaded onto the anion-exchange resin, which made the Fe^{3+}/Fe^{2+} cycle happen at the solid/liquid interface and $HO^{\bullet}$ produced in the homogeneous solution, preventing Q/SQ from deactivation successfully [23].

Being non-toxic, edible, and chemically stable, β-CD possesses a hydrophilic outer surface and a fairly hydrophobic inner cavity with suitable size [24], which is suitable for the inclusion of various organic molecules by formation of a reversible host–guest complex [25]. Cyclodextrin complexation reactions are adopted in many applications like drug delivery system technology, and the reactions are frequently used to the separation and food industries [26]. If selected as catalyst container, β-CD may provide advantages of microheterogeneous reaction [23] in inner-cavity in homogeneous system. In this study, β-CD was selected to coat 2,5-DBQ to explore a cavity-confined reaction category of β-CD-benzoquinone host–guest complex (CDBQ): β-CD provided microreaction space, and 2,5-DBQ catalyzed the iron cycle within the β-CD's cavity, which protected and enhanced the catalytic activity of 2,5-DBQ for the redox cycle of Fe^{3+}/Fe^{2+} in reaction solution under visible irradiation.

Fenton and Fenton-like processes are promising water treatment technologies, due to their high performance, simplicity, and low cost of the reagents [27,28]. The key free radical chain is outlined below [14,22], and the slow reaction [Eq. (2)] is the rate-determination step in Fenton system.

$$Fe^{2+} + H_2O_2 \rightarrow Fe^{3+} + HO\bullet + OH^- \quad k_1 = 76\ M^{-1}S^{-1} \tag{1}$$

$$Fe^{3+} + H_2O_2 \rightarrow Fe^{2+} + HO_2\bullet + H^+ \quad k_2 = 0.02\ M^{-1}S^{-1} \tag{2}$$

Any factor that promotes the reduction of Fe^{3+} to Fe^{2+} would promote the Fenton reaction. Consequently, the CDBQ's cavity-confined acceleration of iron cycle under visible irradiation, in comparison with the

* Corresponding authors.
E-mail addresses: majia@ucas.ac.cn (J. Ma), xfhu@yic.ac.cn (X. Hu).

http://dx.doi.org/10.1016/j.catcom.2015.02.012
1566-7367/

control Fenton system and Fenton system with sacrificial 2,5-DBQ, greatly promoted the Fenton degradation of dye pollutants.

2. Experimental

2.1. Materials

5,8-Dihydroxy-naphthoquinone and 2,5-dihydroxy-1,4-benzoquinone were purchased from J&K. Anthraquinone-1,5-disulfonic acid sodium salt, anthraquinone-2,6-disulfonic acid sodium salt, 5,5-dimethyl-1-pyrroline-N-oxide (DMPO) and β-cyclodextrin were purchased from TCI. Benzoquinone was purchased from Alfa Aesar. Malachite green (MG), Rhodamine B (RhB), hydrogen peroxide, $Fe(ClO_4)_3$, $HClO_4$, ethylenediaminetetraacetic acid sodium salt (EDTA), $FeSO_4 \cdot 7H_2O$, 1,10-phenanthroline, methanol, HAc, NaAc, NaF, H_2SO_4, $AgSO_4$ and $K_2Cr_2O_7$ were of analytical grade. Milli-Q water was used throughout this study. All CDBQ samples used in this study were prepared by a simple process: an appropriate amount of 2,5-DBQ solid was dissolved into the equal molar β-CD solution. For example, CDBQ in Fig. S4 was prepared by adding 0.01135 g β-CD (10^{-5} mol) and 0.0014 g 2,5-DBQ (10^{-5} mol) solids into 50 mL water.

2.2. Reaction systems

All experiments were conducted in aerated solutions in a cylindrical Pyrex vial (10 or 50 mL) under visible irradiation (500 W Xe lamp, with a cut-off filter placed outside the Pyrex jacket to completely remove wavelengths shorter than 420 nm). The initial pH around 2.9 was adjusted with $HClO_4$. Reaction solutions were freshly prepared from stock solution of $Fe(ClO_4)_3$ (1 mM) and dye (0.1 mM).

2.3. Analysis

The degradation of dye MG was determined by UV/Vis spectroscopy (UV-2550, SHIMADZU). Fe^{2+} concentration was determined by 1,10-phenanthroline method (monitored at 510 nm), with excess F^- to suppress any further reduction of Fe^{3+} after reaction.

An AB Sciex QTrap 4500 tandem mass spectrometer (Foster City, Ca, USA) operated with a turbo-V IonSpray source was used to obtain the mass spectra. IronSpray voltage and declustering potential were set to 4.5 keV and 60 eV in the negative ion mode. The sample solution was directly injected into the ESI source. The CDBQ solution, in this analysis, was mixed with 50% methanol before injection. ^1H NMR spectra were recorded on a Bruker Avance III 500 MHz instrument in D_2O at 296.5 K.

The electron paramagnetic resonance (EPR) experiments were recorded on a Bruker ER200D-SRC X-band spectrometer equipped with a 100 kHz field modulation, and the magnetic fields were calibrated by using a Bruker ER 035 M NMR Gaussmeter. The experimental temperature of 123 K or 298 K was controlled by a Bruker ER 4111VT variable temperature unit. The EPR (123/298 K) instrument was operated in the following parameters: microwave power 4.00000/0.99800 mW, microwave frequency 9044.066 MHz/0.99800 mW, sweep time 240.0/30.0 s, center field 323.2/323.1 mT, sweep width 7.5 * 1/5 * 1 mT and 4096/4096 data points.

The X-ray photoelectron spectroscopy (XPS) analysis was performed on a Thermo Scientific ESCALAB 250Xi using Al Kα radiation. The solid samples in XPS experiment were prepared with free-drying. The micro-Raman spectroscopy was performed on a Renishaw inVia plus, and it carried out under ambient conditions by using an argon ion laser (λ = 514.5 nm). Fourier transform infrared spectroscopy (FTIR) was performed on a Bruker VERTEX 70. All the solid samples for FTIR were prepared as the notes in Fig. 1 in liquid, and then treated the liquid sample with freeze-drying for 36 h.

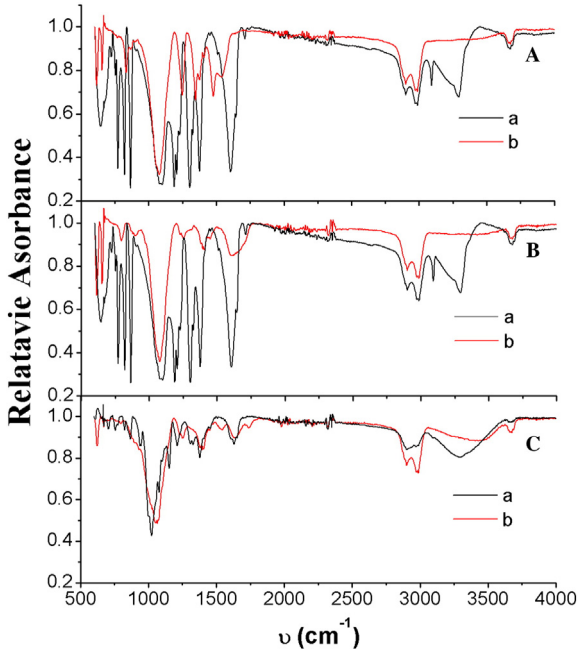

Fig. 1. (A) Infrared spectra of (a) 2,5-DBQ and (b) 2,5-DBQ mixed with Fe^{3+}: 7.5 mM $Fe(ClO_4)_3$, 7.5 mM 2,5-DBQ. (B) Infrared spectra of (a) 2,5-DBQ and (b) 2,5-DBQ reacted with Fe^{3+}/H_2O_2 for 5 min: 7.5 mM $Fe(ClO_4)_3$, 75 mM H_2O_2, 7.5 mM 2,5-DBQ. (C) Infrared spectra of (a) CDBQ and (b) CDBQ reacted with Fe^{3+}/H_2O_2 for 10 min: 7.5 mM $Fe(ClO_4)_3$, 75 mM H_2O_2, 7.5 mM 2,5-DBQ. All the reactions were proceeded at pH = 2.9 under visible irradiation.

3. Results and discussion

3.1. Choice in guest molecule of β-CD

Owing to the corresponding reduction ability for Fe^{3+} under irradiation, five quinones were selected as guests of β-CD, including 5,8-dihydroxy-naphthoquinone, anthraquinone-1,5-disulfonic acid sodium salt, benzoquinone, 2,5-dihydroxy-1,4-benzoquinone, anthraquinone-2,6-disulfonic acid sodium salt. Then the catalytic activity of these quinones was studied by comparing their degradation of MG in Fenton-like reaction under visible irradiation. Fig. S1 revealed that 2,5-DBQ was the best co-catalyst in the photo-Fenton reaction among the five quinones, so 2,5-DBQ was selected as β-CD's guest molecule.

A result from a typical titration experiment monitored by ^1H NMR was showed in Fig. S2. This figure showed how the β-CD protons shift in the presence of varying amounts of 2,5-DBQ. The downfield shifts of H-3′ and H-5′ were obvious, and the band shape alteration of H-5′ was apparent. H-3′ and H-5′ are the protons located in the interior of the cavity. The significant modifications of these protons are usually considered as a support for the complexation process [29,30]. This observation indicated that 2,5-DBQ was included in the β-CD cavity.

The successful coating was also evidenced by ESI-MS. In Fig. S3, the ion corresponding to the CDBQ's supramolecular complex was clearly observed, compared with those corresponding to uncomplexed β-CD and 2,5-DBQ in the mass spectra. For the complex of β-CD with 2,5-DBQ, the ion at m/z 1273 corresponded to $[CDBQ–H]^-$, and the ion at m/z 1133 and 139 were also assigned as the peak corresponding to $[β\text{-CD–H}]^-$ and $[2,5\text{-DBQ–H}]^-$. The results confirmed the supramolecular interactions between β-CD and 2,5-DBQ.

3.2. The function of β-CD for iron cycle

Fe^{3+} is more thermodynamically stable than Fe^{2+} in most environmental and chemical systems. Therefore, the key to attain Fe^{3+}/Fe^{2+} effectively proceeding is to substantially enhance the Fe^{3+} reduction rate.

CDBQ's acceleration for iron cycle was explored in Fenton-like system, comparing with uncoated 2,5-DBQ. Fig. S4 showed the Fe^{2+} yield in different systems. In comparison with the control Fenton reaction (Fig. S4, curve c), much more Fe^{2+} were produced in the presence of CDBQ under visible irradiation—tower above 85% of the total iron content at 15 minute reaction time (Fig. S4, curve a). More notably, in photo-Fenton system with 2,5-DBQ as co-catalyst, although the Fe^{2+} yield was higher than the control Fenton system, it just remained a fairly low concentration—about 8% of the total iron content (Fig. S4, curve b). These results demonstrated that CDBQ could efficiently reduce Fe^{3+} to Fe^{2+}, even in the presence of H_2O_2, which indicated that CDBQ could recycle Fe^{2+} from Fe^{3+} in Fenton-like reactions. In addition, β-CD coating greatly improved the acceleration of iron cycle by 2,5-DBQ.

In homogeneous Fenton system, quinones will decompose quickly under attack by non-selective HO·[22,23], which is in accordance with the experimental result in curve b in Fig. S4. The Fe^{2+} yield experiments proved that β-CD played a positive and important role in promoting the 2,5-DBQ catalytic activity for iron cycle under visible irradiation. The reaction system with addition of CDBQ, was still a homogeneous system, but with a cavity space, thus how did 2,5-DBQ molecule avoid the attack of $HO^{\bullet}$ in the solution during the reaction? Where did the iron cycle happen? Please see the discussions below.

3.3. Mechanism discussion

Infrared spectra of 2,5-DBQ and iron ions were illustrated in Fig. 1A. 2,5-DBQ has two different coordinated models: (1) All of its carbonyl and hydroxyl groups provide oxygen atoms for coordination. (2) Only two hydroxyl oxygen atoms connect the metal ions and the other two uncoordinated oxygen atoms can be assigned to C═O [31]. The first coordinated model was confirmed by the ν(C═O) shifts that complexation ν(C═O) of the dihydroxybenzoquinone ligand at 1609 cm^{-1} and 1646 cm^{-1} (shoulder peak) decreased to 1475 cm^{-1} in Fe–dihydroxybenzoquinone complex after interacting with Fe^{3+} in Fig. 1A [32,33]. The ν(OH) frequency was sensitive to hydrogen bond interaction, and it was nearly diminished in 3300 cm^{-1}. The results showed that both carbonyl and hydroxyl oxygen atoms coordinated with the iron ions when 2,5-DBQ reacted with Fe^{3+}. The coordination of the iron ions to the quinone oxygen atoms of 2,5-DBQ molecule was deduced from the weakening of the C═O bond in Raman spectra as well [33], which was in accordance with the result of FTIR.

In Fig. 1B, the comparison of infrared spectra of 2,5-DBQ with 2,5-DBQ anticipating Fenton reaction demonstrated that the initial structure of 2,5-DBQ came back after anticipating the Fenton reaction. Upon complexation, ν(C═O) of the Fe-dihydroxybenzoquinone complex at 1475 cm^{-1} (Fig. 1B, b) went back to 1609 cm^{-1} again, and the same as CDBQ did in Fig. 1C. Therefore, 2,5-DBQ reacted with Fe^{3+} to give Fe–dihydroxybenzoquinone complex, and the complex recovered to the original quinone unit structure after altering the iron cycle pathway.

The catalytic mechanism of CDBQ in Fenton reaction was further deduced by analyzing C_{1s} spectrums of CDBQ-XPS sample and CDBQ & Fenton sample (CDBQ-XPS sample anticipating Fenton-like reaction). In Fig. S5, the C_{1s} spectrums of 2,5-DBQ and CDBQ all displayed two peaks at 284.7 [34] and 286.4, corresponding to the carbon atoms in benzene ring-C and C═O of quinone. Comparing the Fig. S5(A) and (B), a negligible proportion (~4%) transformed from C═O of quinone into benzene ring-C. The results revealed the chemical structure of 2,5-DBQ had few change with β-CD protection after participating Fenton-like reaction, which corresponded to the proofs from FTIR.

EPR is an effective technique to detect the generation of radicals or radical intermediates. Photoexcitation of quinone leads to efficient production of a semi-quinone-like (SQ) radical by apparent one-photon photooxidation of water [35]. SQ radical signal was generally detected in organic phase, and only in very rare cases was it detected in aqueous solution. Here, the EPR experiment (123 K) captured the strength increase of SQ radical signal over time in aqueous solution under visible irradiation. In Fig. 2, there was no SQ radical signal in the absence of visible irradiation. However, the signal became obvious when the reaction solution was illuminated for 10 min, and it got stronger at 20 min irradiation. The results confirmed the generation of SQ radical whose signal was increasing as reaction proceeding due to photoexcitation of CD-protected quinones. The intermediate products of 2,5-DBQ have not been detected by LC-MS as a result of the extremely unstable of OH-Q [14].

Based on the above discussions, we suggested that SQ radical could coordinate with iron ions, and then the radical as an electron donor shuttled one electron to Fe^{3+} by complex forming. With reduction of Fe^{3+}, the SQ radical itself was oxidized to original quinone form [Eq. (5)], and prepared for the next catalysis cycle under visible irradiation. Hence, to clearly explore the mechanism, it is important to figure out where did the redox of quinones with Fe^{2+}/Fe^{3+} happen. As known, the attack of active radical will result in the deactivation of unprotective quinones in Fenton system while the system has the highest $HO^{\bullet}$ concentration around Fe^{2+} in bulk solution, thus it is impossible that the redox occur in bulk solution. It had been proved that β-CD protected quinones against active radicals' attacking, hence the redox could only occur within the β-CD's cavity or at the CD/solution interface, but could not be possible in bulk solution. As no signals corresponding to Fe_{2p} were detected in XPS experiments for either "fresh" or "used" CDBQ samples, it denied the possibility of the interface, therefore, it was reasonable that the Fe^{2+}/Fe^{3+} redox cycle occurred within β-CD's cavity. Hydroxyl radical is generated in bulk solution with limited lifetime, which means the diffusion range is fairly short. Hydroxyl radical will superiorly attack the organic substrate in homogenous solution, so there are few chances for hydroxyl radical to attack the 2,5-DBQ within the β-CD's cavity.

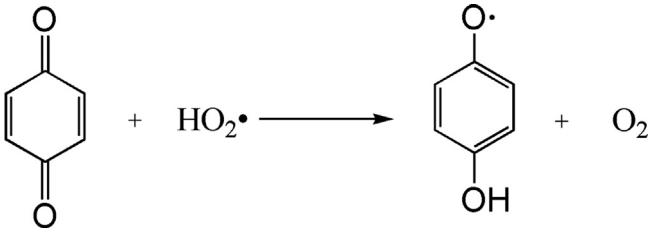

(3)

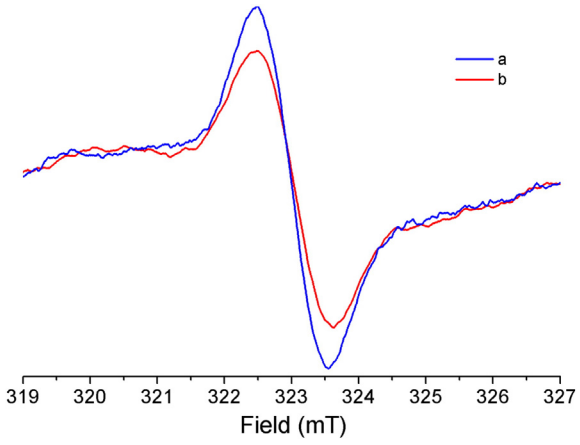

Fig. 2. EPR spectra (123 K) of the generated SQ radical at different reaction times: a) 20 min, b) 10 min, initial concentrations: 0.2 mM $Fe(ClO_4)_3$, 3 mM CDBQ, pH = 2.9, under visible irradiation.

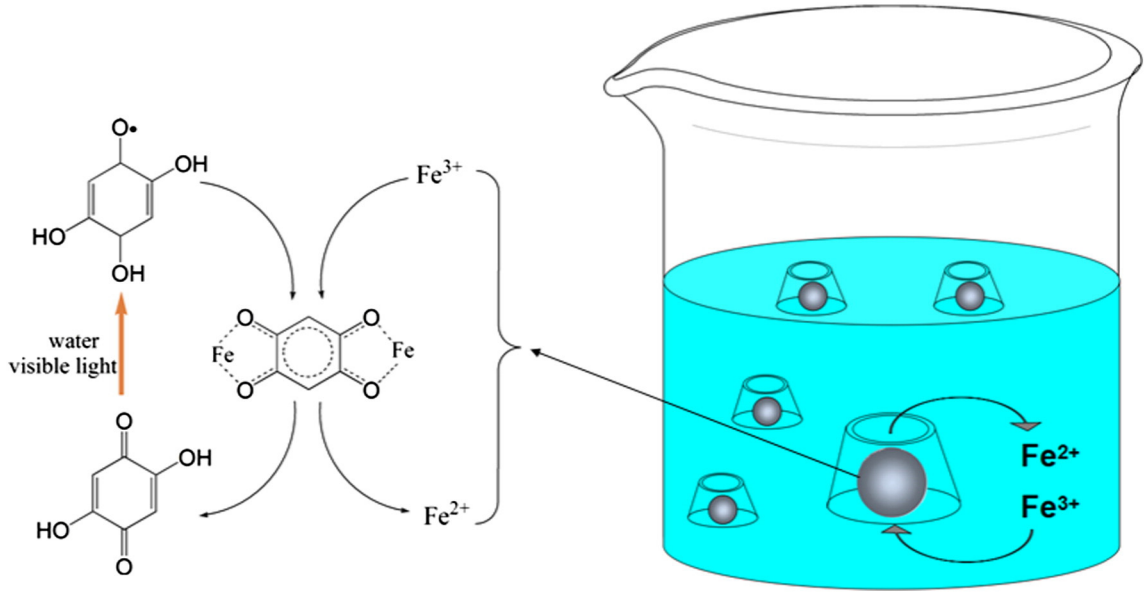

Scheme 1. Cavity-confined acceleration of iron cycle by CDBQ under visible irradiation.

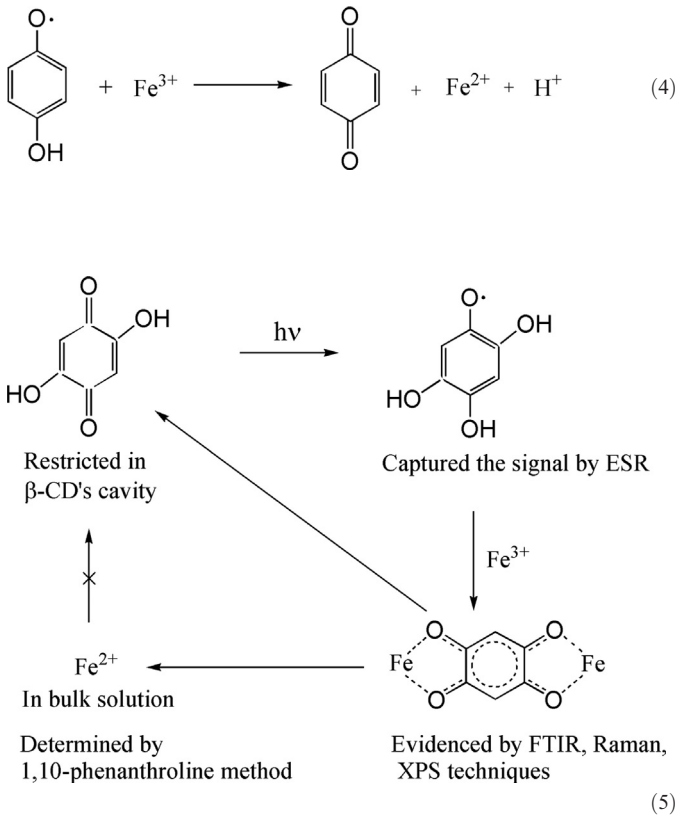

$$\text{Fe}^{3+} + \text{H}^{+} \quad (4)$$

(5)

From the above discussion, the mechanism showed in Scheme 1 is proposed for cavity-confined acceleration of iron cycle by CDBQ under visible irradiation.

3.4. CDBQ's acceleration for Fenton degradation of dyes

From the results obtained, it can be concluded that adding CDBQ into Fenton system can accelerate the iron cycle effectively, furthermore, the catalytic capability of CDBQ is more effective than 2,5-DBQ in accelerating iron cycle for photo-Fenton reaction. The CDBQ's co-catalytic activity for Fenton degradation of MG was excellent and maintained efficient even in the presence of EDTA as an extreme complexant that could strongly complex the iron species ($E°(Fe^{3+}/Fe^{2+}$—EDTA) = 0.12 V vs NHE) [14]. In Fig. 3A, MG degraded over 80% in Fenton-CDBQ system under visible irradiation after reacting 150 min, while the dye had no significant degradation in parallel control system. For the cycle experiment (Fig. 3A, inset), the co-catalytic activity of CDBQ in the degradation of MG maintained efficient after 24 recycle and the turnover number for CDBQ against dye was about 10. The recycle experiment of Fenton-CDBQ system showed that the degradation rate started slowly and then speeded up at first (stage 1, cycle 1–cycle 7), and then stabilized (stage 2, cycle 8–cycle 16), and the rate reduced for the last stage (stage 3, cycle 17–cycle 24). According to the monitoring data of pH value in recycle experiment (Fig. 3B), the decrease of degradation rate

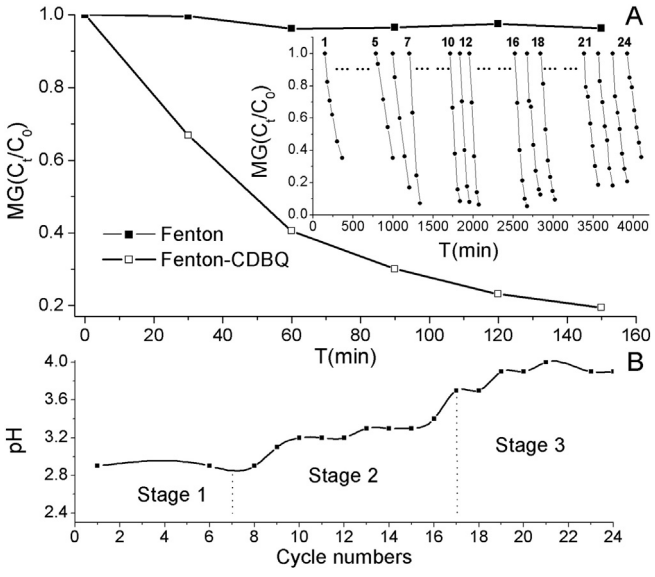

Fig. 3. (A) Fenton degradation of MG with CDBQ: 0.5 mM EDTA, 0.15 mM MG, 2 mM H_2O_2, 0.2 mM CDBQ, 0.2 mM $Fe(ClO_4)_3$, pH = 2.9, visible irradiation. Inset: cyclic degradation of MG (50 mL): CDBQ and Fe^{3+} repeatedly used, supply 0.08 mM MG and 0.2 mM H_2O_2/run. (B) The pH value of three stages for cyclic degradation of MG.

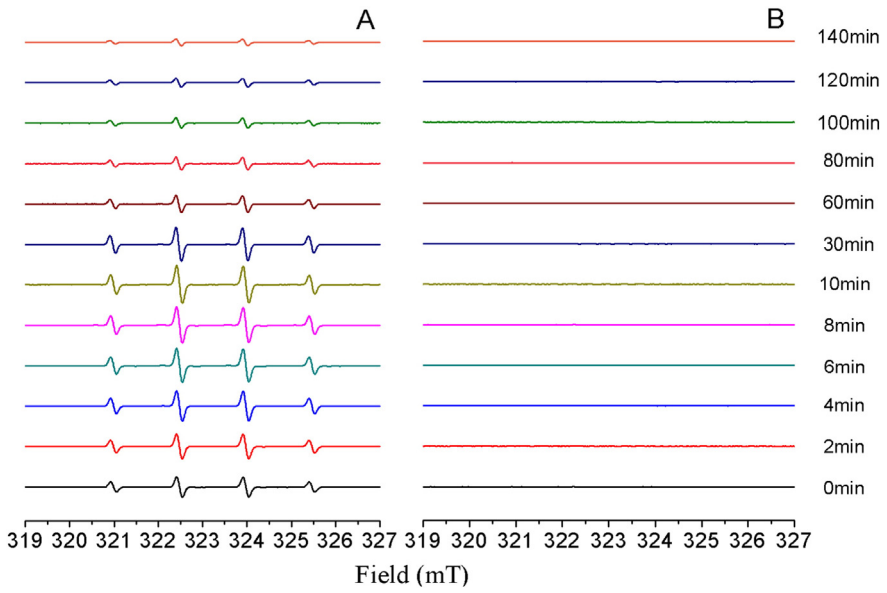

Fig. 4. EPR spectra of the generated DMPO-HO• in CDBQ and control systems: 0.2 mM $Fe(ClO_4)_3$, 4 mM H_2O_2, pH = 2.9, visible irradiation, with or without 0.2 mM CDBQ (A or B).

in stage 3 could be attributed to the increase in pH, and the initial induction period [22] of hydroquinone/quinone could be the reason for the slow degradation rate in stage 1. These aforementioned results demonstrated that CDBQ system exhibited high catalytic activity to accelerate the MG degradation in the Fenton reaction after an induction period, and the photoreaction over CDBQ was a catalytic process rather than a stoichiometric one. Another organic dye RhB showed the similar results to MG in the three groups.

HO• is a very strong and nonselective oxidant capable of degrading a wide array of pollutants and its amount roughly represents the Fenton reaction rate. The photocatalytic activity of CDBQ in Fenton-like system was tested by comparing the HO• yield between CDBQ system and control system in Fig. 4, utilizing DMPO spin trapping EPR technique to measure the signal of DMPO-•OH. In Fig. 4, the intensity of DMPO-•OH signals in Fenton-CDBQ system were strong and obviously increased as irradiation proceeding, conversely, the signals were rather poor and had no response to visible light in control system. The dramatic difference of the two groups illustrated the photocatalytic activity of CDBQ. The CDBQ could remarkably enhance HO• yield and activate Fenton system's response to visible light, hence it promoted the degradation of pollutants under visible irradiation. A kinetic study on the yield of HO• in the absence of hydrogen peroxide was also performed, and the HO• signals that were promoted by CDBQ and H_2O were detected, but the signals were weaker than the counterpart with hydrogen peroxide and had no response to visible light. The results demonstrated that CDBQ increased the HO• yield by accelerating cavity-confined iron cycle.

4. Conclusion

Cavity-confined acceleration of iron cycle is ultimately achieved through readily available β-CD-benzoquinone host–guest complex under visible irradiation, which promotes the Fenton-like degradation of pollutants in water. The acceleration is a catalytic reaction with highly active and stable features, and notably, β-CD is an environmentally friendly chemical. The reported strategy could be promising for improving the efficiency of photo-Fenton processes in pollutant degradation and wastewater remediation, and such a cavity-confined reaction may also be used in other catalytic systems.

Acknowledgments

This work was supported by the NSFC (nos. 21007089 and 21377126) and the SRF for ROCS, SEM of China.

Appendix A. Supplementary data

Supplementary data to this article can be found online at http://dx.doi.org/10.1016/j.catcom.2015.02.012.

References

[1] W. Arabczyk, I. Jasinska, R. Jedrzejewski, Catal. Commun. 10 (2009) 1821–1823.
[2] G.S. Ananthnag, A. Adhikari, M.S. Balakrishna, Catal. Commun. 43 (2014) 240–243.
[3] S. Gorelik, J. Kanner, J. Agric. Food Chem. 49 (2001) 5939–5944.
[4] G. Zhuang, Y. Zhen, R. Duce, P. Brown, Nature 355 (1992) 537–539.
[5] C. Brandt, I. Fa'bia'n, R. Eldik, Inorg. Chem. 33 (1994) 687–701.
[6] S. Hug, O. Leupin, Environ. Sci. Technol. 37 (2003) 2734–2742.
[7] M. Gaberell, Y. Chin, S. Hug, B. Sulzberger, Environ. Sci. Technol. 37 (2003) 4403–4409.
[8] X. Liu, F. Wu, N. Deng, Environ. Sci. Technol. 38 (2004) 296–299.
[9] D. King, H. Lounsbury, F. Millero, Environ. Sci. Technol. 29 (1995) 818–824.
[10] B. Southworth, B. Voelker, Environ. Sci. Technol. 37 (2003) 1130–1136.
[11] B. Faust, R. Zepp, Environ. Sci. Technol. 27 (1993) 2517–2522.
[12] H. Xie, O. Zafiriou, W. Cai, R. Zepp, Y. Wang, Environ. Sci. Technol. 38 (2004) 4113–4119.
[13] M. Elsner, R. Schwarzenbach, S. Haderlein, Environ. Sci. Technol. 38 (2004) 799–807.
[14] M. Tokumura, R. Morito, R. Hatayama, Y. Kawase, Appl. Catal. B Environ. 106 (2011) 565–576.
[15] P. Behra, L. Sigg, Nature 344 (1990) 419–421.
[16] M. Rijkenberg, A. Fischer, J. Kroon, L. Gerringa, K. Timmermans, H. Wolterbeek, H. Baar, Mar. Chem. 93 (2005) 119–129.
[17] L. Chen, J. Ma, X. Li, J. Zhang, J. Fang, Y. Guan, P. Xie, Environ. Sci. Technol. 45 (2011) 3925–3930.
[18] Y. Segura, F. Martínez, J. Melero, R. Molina, R. Chand, D. Bremner, Appl. Catal. B Environ. 113–114 (2012) 100–106.
[19] Y. Adewuyi, Environ. Sci. Technol. 39 (2005) 3409–3420.
[20] R. Chen, J.J. Pignatello, Environ. Sci. Technol. 31 (1997) 2399–2406.
[21] F. Chen, J. He, J. Zhao, J. Yu, New J. Chem. 26 (2002) 336–341.
[22] J. Ma, W. Song, C. Chen, W. Ma, J. Zhao, Y. Tang, Environ. Sci. Technol. 39 (2005) 5810–5815.
[23] J. Ma, W. Ma, C. Chen, H. Ji, J. Zhao, Chem. Asian. J. 6 (2011) 2264–2268.
[24] Y. Huang, W. Ma, J. Li, M. Cheng, J. Zhao, L. Wan, J.C. Yu, J. Phys. Chem. B 107 (2003) 9409–9414.
[25] Q. Hu, G. Tang, P. Chu, Acc. Chem. Res. 47 (2014) 2017–2025.
[26] M.V. Rekharsky, Y. Inoue, Chem. Rev. 98 (1998) 1875–1917.
[27] S. Wang, Dyes Pigments 76 (2008) 714–720.
[28] H. Lee, M. Shoda, J. Hazard. Mater. 153 (2008) 1314–1319.

[29] D. Salvatierra, C. Jaime, A. Virgili, F. Sanchez-Ferrando, J. Org. Chem. 61 (1996) 9578–9581.
[30] K. Eliadou, K. Yannakopoulou, A. Rontoyianny, I.M. Mavridis, J. Org. Chem. 64 (1999) 6217–6226.
[31] J. Xiang, C. Chang, M. Li, S. Wu, L. Yuan, J. Sun, Cryst. Growth Des. 8 (2008) 280–282.
[32] J. Wrobleski, D. Brown, Inorg. Chem. 18 (1979) 2739–2749.
[33] T. Demars, M. Boltoeva, N. Vigier, J. Maynadié, J. Ravaux, C. Genre, D. Meyer, Eur. J. Inorg. Chem. 24 (2012) 3875–3884.
[34] X. He, X. Wang, X. Jin, H. Zhou, X. Shi, G. Chen, Y. Long, J. Am. Chem. Soc. 133 (2011) 3649–3657.
[35] S. Beck, L. Brus, J. Am. Chem. Soc. 104 (1982) 1103–1104.